Intermittent hypoxia in obstructive sleep apnoea mediates insulin resistance through adipose tissue inflammation

Aoife M. Murphy[1], Amandine Thomas[2], Sophie J. Crinion[3], Brian D. Kent[4], Murtaza M. Tambuwala[5], Aurelie Fabre[6,7], Jean-Louis Pepin[2], Helen M. Roche[1], Claire Arnaud[2] and Silke Ryan[3,8]

Affiliations: [1]Nutrigenomics Research Group, School of Public Health, Physiotherapy and Sports Science, Conway Institute, University College Dublin, Dublin, Ireland. [2]Université Grenoble Alpes, HP2, Inserm, U1042, CHU de Grenoble, Laboratoire EFCR, Pôle Thorax et Vaisseaux Grenoble, Grenoble, France. [3]Pulmonary and Sleep Disorders Unit, St Vincent's University Hospital, Dublin, Ireland. [4]Pulmonary and Sleep Disorders Unit, Guy's and St Thomas' Hospital, London, UK. [5]School of Pharmacy and Pharmaceutical Science, Ulster University, Coleraine, UK. [6]Dept of Pathology, St Vincent's University Hospital, Dublin, Ireland. [7]Research Pathology Core Technology, Conway Institute, University College Dublin, Dublin, Ireland. [8]School of Medicine, Conway Institute, University College Dublin, Dublin, Ireland.

Correspondence: Silke Ryan, Dept of Respiratory Medicine, St Vincent's University Hospital, Elm Park, Dublin 4, Ireland. E-mail: silke.ryan@ucd.ie

@ERSpublications
Intermittent hypoxia induces inflammatory phenotype of adipose tissue leading to insulin resistance in sleep apnoea http://ow.ly/k1TX3091YBM

Cite this article as: Murphy AM, Thomas A, Crinion SJ, *et al*. Intermittent hypoxia in obstructive sleep apnoea mediates insulin resistance through adipose tissue inflammation. *Eur Respir J* 2017; 49: 1601731 [https://doi.org/10.1183/13993003.01731-2016].

ABSTRACT Obstructive sleep apnoea (OSA) is increasingly associated with insulin resistance. The underlying pathophysiology remains unclear but intermittent hypoxia (IH)-mediated inflammation and subsequent dysfunction of the adipose tissue has been hypothesised to play a key role.

We tested this hypothesis employing a comprehensive translational approach using a murine IH model of lean and diet-induced obese mice, an innovative IH system for cell cultures and a tightly controlled patient cohort.

IH led to the development of insulin resistance in mice, corrected for the degree of obesity, and reduced insulin-mediated glucose uptake in 3T3-L1 adipocytes, associated with inhibition of the insulin-signalling pathway and downregulation of insulin-receptor substrate-1 mRNA. Providing mechanistic insight, IH induced a pro-inflammatory phenotype of visceral adipose tissue in mice with pro-inflammatory M1 macrophage polarisation correlating with the severity of insulin resistance. Complimentary *in vitro* analysis demonstrated that IH led to M1 polarisation of THP1-derived macrophages. In subjects without comorbidities (n=186), OSA was independently associated with insulin resistance. Furthermore, we found an independent correlation of OSA severity with the M1 macrophage inflammatory marker sCD163.

This study provides evidence that IH induces a pro-inflammatory phenotype of the adipose tissue, which may be a crucial link between OSA and the development of insulin resistance.

This article has supplementary material available from erj.ersjournals.com

Received: Aug 31 2016 | Accepted after revision: Dec 20 2016

Support statement: This work was supported by the Health Research Board of Ireland (S. Ryan), the Science Foundation of Ireland (H.M. Roche and A.M. Murphy) and by Agir pour les maladies chroniques (J-L. Pepin). The murine studies were partly supported by the French National Research Agency in the framework of the "Investissements d'avenir" programme (ANR-15-IDEX-02). Funding information for this article has been deposited with the Crossref Funder Registry.

Conflict of interest: None declared.

Introduction

Obstructive sleep apnoea (OSA) represents a major public health burden because of its high prevalence [1] and substantial association with cardiovascular morbidity and mortality [2, 3]. Furthermore, there is emerging evidence of a relationship between OSA and metabolic perturbations, and in particular with alterations in glucose metabolism leading to insulin resistance (IR) and type 2 diabetes (T2D) [4–8].

Intermittent hypoxia (IH) is likely to play a key role in the pathophysiology of cardiometabolic processes in OSA [9]. We have previously shown that IH preferentially activates pro-inflammatory, nuclear factor (NF)-κB-mediated pathways leading to systemic inflammation in OSA patients [10, 11] and mice [12]. However, the tissues responsible for generating pro-inflammatory mediators in response to IH remain unknown. White adipose tissue (WAT) has emerged as an attractive possibility, given the strong link between OSA and obesity. A hallmark feature of metabolically dysfunctional obese WAT is the infiltration of immune cells, particularly macrophages with polarisation towards a pro-inflammatory M1 phenotype and formation of crown-like structures (CLS), which generate a constant low-grade secretion of pro-inflammatory mediators, thereby driving cardiovascular and metabolic disease processes [13]. Emerging evidence suggests that local WAT hypoxia is a key factor in triggering inflammatory adipokine expression in obesity [14, 15]; in OSA, IH may potentiate this action. In support of this hypothesis we have demonstrated that primary human adipocytes develop a significantly greater inflammatory response to IH exposure than primary non-adipocyte cells [16]. Furthermore, IH leads to increased secretion of pro-inflammatory adipokines from adipose tissue in apolipoprotein E-deficient mice, associated with the development of more severe atherosclerotic lesions than seen in control mice [17].

However, the detailed mechanisms of the interaction between OSA and obesity and the specific role of WAT in the development of metabolic conditions such as IR in OSA remain poorly understood. Thus, we hypothesised that IH contributes to the pathogenesis by inducing morphological and functional changes of the adipose tissue promoting an inflammatory response. We tested the hypothesis using a comprehensive translational approach employing a murine model of IH, a state-of-the-art IH system for cell cultures and a large human study including well-phenotyped subjects free of comorbidities.

Methods

Detailed methods are described in the supplementary material.

Mice

Male C57Bl/6 mice (5 weeks old) were either fed a high-fat diet or matched low-fat diet for 14 weeks before randomisation to IH (21–5% inspiratory oxygen fraction, 60-s cycle, 8 h per day) as previously described [17] or control for 6 weeks. Upon completion of the protocol, the intraperitoneal insulin tolerance test (ITT) was performed [17]. Epididymal adipose tissue (EAT) was harvested, processed immediately for isolation of the stromal vascular fraction, culture or *ex vivo* insulin stimulation or stored for further analysis. Flow cytometry of the stromal vascular fraction was performed to quantify the M1 and M2 fraction of the adipose macrophage population, and F4/80 immunohistochemistry was performed to determine the CLS density. The study was approved by the Institutional Animal Care and Use Committee (#02256.02) and mice were maintained in accordance with the European Convention for the Protection of Vertebrate Animals used for Experimental and other Scientific Purposes.

Human studies

A total of 186 male subjects without significant comorbidities were recruited from St Vincent's University Hospital, Dublin, Ireland, and University Hospital, Grenoble, France. The study was approved by the local ethics committees and all participants gave written informed consent. Polysomnography (PSG) was performed as previously described [10]. Fasting glucose, insulin and lipid profile were determined and circulating levels of sCD163 were measured by ELISA (R&D, Abingdon, UK). The homeostasis model assessment resistance index (HOMA-IR) was calculated by the equation: insulin ($mU \cdot L^{-1}$)×glucose ($mmol \cdot L^{-1}$)/22.5.

In vitro *model of IH*

Previous cell culture models of IH have been limited by requiring prolonged soak times, reduced cycle numbers and inadequate control treatment. Here, we have developed a state-of the art model using a custom-built system (Coy Laboratories, Grass Lake, MI, USA) overcoming these limitations. Cells were grown on a semi-permeable membrane (Lumox®; Sarstedt, Nuermbrecht, Germany) to allow rapid gas exchange. IH and control treatment were achieved in two separate closed cabinets with gas flow simultaneously regulated by an automated external controller (Coy Laboratories). The IH protocol consisted of alternating cycles of 40 s of 16% O_2/5% CO_2/balance N_2 and 40 s of 3% O_2/5% CO_2/balance N_2. The protocol was applied for 8 h per day for 3 consecutive days. The actual partial pressure of oxygen values in the cell monolayer were continuously monitored by fluorescence quenching oxymetry (Oxylite

2000; Oxford Optronix, Abingdon, UK). The control chamber was simultaneously cyclically gassed with 16% O_2/5% CO_2/balance N_2. Both chambers were kept in a closed glove box, maintaining the temperature at 37°C with separate heat exchangers to ensure a constant temperature in the IH and control cabinets.

Cell culture

3T3-L1 cells were differentiated into mature adipocytes according to the manufacturer's instructions. NIH-3T3 cells (Panomics, Cambridge, UK) stably transfected with a NF-κB-luciferase reporter construct were maintained in complete DMEM supplemented with hygromycin (100 μg·mL^{-1}) (Roche, Clare, Ireland). Human monocytic THP1 cells (ATCC) were differentiated into macrophages using 5 ng·mL^{-1} phorbol 12-myristate 13-acetate (PMA, Sigma) for 48 h before resting in medium for 72 h. Then, cells were either left unstimulated or incubated with interferon (IFN)-γ (20 ng·mL^{-1}, R&D) or lipopolysaccharide (LPS) (1 ng·mL^{-1}, Sigma) for 24 h.

Statistical analysis

All data are expressed as mean±SD or mean±SEM as indicated. Group comparison was performed using one-way ANOVA followed by Bonferroni *post hoc* comparison. To assess the possible confounding effect of weight on IR in the mice experiment, a general linear model to assess for ANCOVA was employed. To identify potential independent predictors of HOMA-IR or sCD163, we used a stepwise linear regression model with HOMA-IR or sCD163 as the dependent variables and baseline demographic, anthropometric, and PSG variables as covariates. A p-value of <0.05 was considered statistically significant. Statistical analysis was performed using a commercial software package (SPSS Version 20, Chicago, IL, USA).

Results

IH induces insulin resistance in lean and obese mice and impedes insulin-mediated glucose uptake in adipocytes

Previous studies have linked IH to IR in mice but limited data are available in the setting of obesity. Here, using the murine diet-induced obesity model, we exposed lean and obese mice to IH or control conditions.

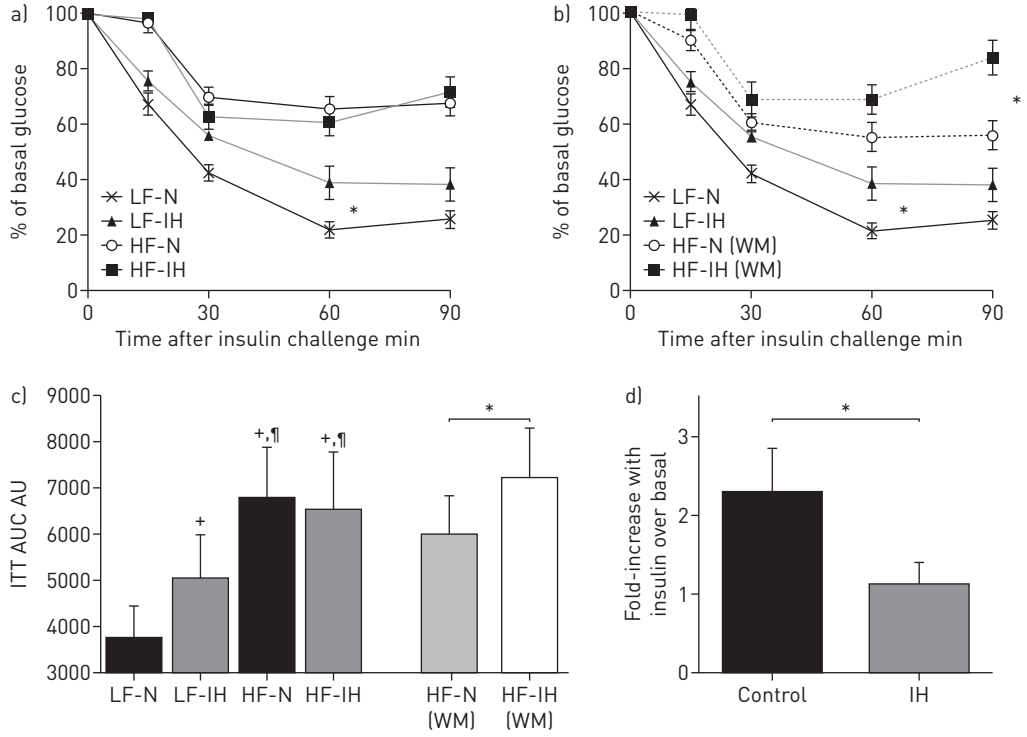

FIGURE 1 Intermittent hypoxia (IH) leads to insulin resistance in lean and diet-obese mice and impedes insulin-mediated glucose uptake in adipocytes. Lean (LF) and diet-induced obese (HF) mice were treated with IH or control (N) for 6 weeks. Intraperitoneal insulin tolerance test (ITT) was performed following 6 h fasting. a) ITT represented for the whole, un-matched cohort (n=10–13 per group). b) ITT represented for the cohort with obese mice matched for body weight (WM) (n=7 per group). c) Area under the curves (AUC). Data are presented as mean±SD. *: p<0.05; $^{+}$: p<0.05 *versus* LF-N; ¶: p<0.05 *versus* LF-IH. Next, we investigated the impact of IH on cultured adipocytes. 3T3-L1 adipocytes were exposed to alternating cycles of 40 s of 16% O_2/5% CO_2/balance N_2 and 40 s of 3% O_2/5% CO_2/balance N_2 for 8 h per day for 3 consecutive days (IH) or an identical regimen of 16% O_2/5%CO_2/balanceN_2 (control). Insulin-stimulated ^{3}H-glucose transport was subsequently monitored. d) Fold change relative to basal glucose uptake is presented. n=4; data are presented as mean±SD. *: p<0.05.

IH had a clear adverse effect upon IR in lean and weight-matched obese mice as demonstrated by the ITT (figure 1a–c). In obese mice, as expected, IH-treated animals lost significantly more weight than controls (table 1). Therefore, all of the IR measures took account of this confounding effect and results are presented for the whole cohort of obese mice (figure 1a) and separately for weight-matched animals (figure 1b). Weight matching was performed by excluding mice with the highest and the lowest body weights; matching was performed prior to statistical analysis by an investigator blinded to any obtained results (M.M. Tambuwala). Furthermore, using ANCOVA with body weight as the covariate, IH treatment remained a significant predictor of IR ($p<0.001$).

Obese mice displayed higher fasting insulin levels and HOMA index and demonstrated impaired glucose tolerance than lean mice ($p<0.05$), but this was not further altered by IH treatment.

To gain mechanistic insight into IH-induced IR, we utilised a state-of-the-art *in vitro* model of IH. This model results in rapid fluctuations of cellular partial pressure of oxygen closely mimicking the IH pattern experienced by OSA patients (supplementary figure E1). In cultured 3T3-L1 adipocytes, IH treatment significantly attenuated insulin-mediated glucose uptake compared with control treatment (figure 1d).

Taken together, these results indicate that IH leads to decreased insulin sensitivity in lean and obese mice as well as cultured adipocytes.

IH inhibits the insulin signalling pathway and downregulates IRS-1 in mice and cultured adipocytes

Having established the direct link between IH and IR, we next investigated potential upstream events. In obesity, downregulation of insulin-receptor substrate (IRS)-1 mRNA with subsequent alteration in IRS-1 tyrosine phosphorylation and diminished phosphorylation of Akt have been recognised as important components of IR [18], and, here, we examined the impact of IH on these events. In both, murine epididymal visceral fat and 3T3-L1 adipocytes, IH reduced IRS-1 mRNA, although this did not reach statistical significance in lean mice ($p=0.06$) (figure 2a,b). Murine IRS-1 mRNA correlated significantly with insulin sensitivity as determined by ITT ($r=0.436$, $p=0.021$). Furthermore, IH led to decreased insulin-induced tyrosine-phosphorylation of the insulin receptor (IRβ) and IRS and phosphorylation of Akt (figure 2c) in adipocytes. In addition, in adipose explants of obese mice, *ex vivo* insulin stimulation also resulted in attenuated Akt phosphorylation (figure 2d) (given the limited amount of adipose tissue this experiment was not performed in lean mice).

Thus, IH leads to decreased functionality of the adipose tissue with inhibition of the insulin signalling pathway and downregulation of IRS-1 mRNA.

IH induces a pro-inflammatory phenotype in visceral adipose tissue in vivo *and polarises THP1 cells into M1 pro-inflammatory macrophages*

To further understand the mechanisms responsible for the development of the adipose IR phenotype in response to IH, we next examined the effect of IH on pro-inflammatory adipose tissue macrophage (ATM) alteration. Notably, IH was associated with increased M1 (pro-inflammatory) ATM infiltration in lean and obese mice, and M1 ATM numbers correlated significantly with the level of IR as assessed by ITT (figure 3a,b). Percentages of M2 (anti-inflammatory) macrophages were significantly reduced with a high-fat diet, but this was not further altered by IH treatment (figure 3c and supplementary figure E2). Overall, there were no changes in total ATM infiltration between diets and treatments (lean control mice 141±61 *versus* lean IH 102±56 *versus* diet-induced obese control mice 169±141 *versus* diet-induced obese IH mice 176±200 mm^{-2}; ANOVA: $p=0.118$) as determined by automated analysis of F4/80 immunohistochemistry. Another typical

TABLE 1 Baseline characteristics of lean (LF) and diet-induced obese (HF) mice (whole cohort and weight-matched) treated with intermittent hypoxia (IH) or control

	LF		HF (whole cohort)		HF (weight-matched)	
	Control	IH	Control	IH	Control	IH
Mice n	10	10	13	13	7	7
Body weight g day 0 (non-fasting)	29.7±3.6	30.3±2.3	45.0±5.4[¶]	44.5±3.3[¶]	43.9±3.8[¶]	44.6±2.0[¶]
Body weight g day 42 (fasting)	25.2±2.9	25.6±1.7	42.0±5.1[¶]	35.1±3.3[#,¶]	38.2±3.6[¶]	37.6±1.8[¶]
Epididymal fat g	0.446±0.124	0.534±0.139	2.002±0.556[¶]	1.689±0.532[¶]	2.013±0.464[¶]	1.903±0.548[¶]

[#]: $p<0.05$ *versus* HF control; [¶]: $p<0.05$ *versus* LF control and LF-IH.

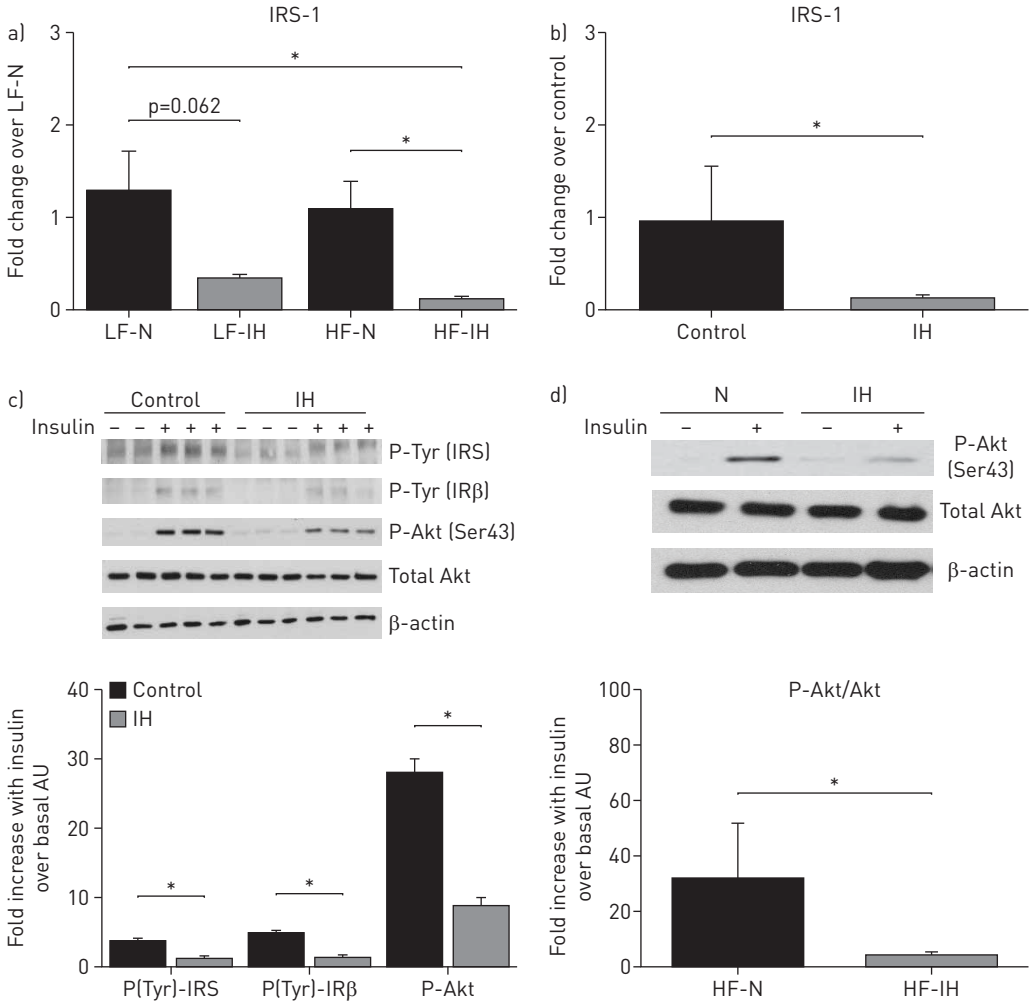

FIGURE 2 Intermittent hypoxia (IH) downregulates insulin-receptor substrate (IRS)-1 mRNA in mice and cultured adipocytes and inhibits the insulin signalling pathway. mRNA of epididymal adipose tissue of lean (LF; n=6 per group) and obese mice (HF; n=8 per group) (a) and cultured 3T3-L1 adipocytes (n=4) (b) following treatment with IH or control (N) was harvested and IRS-1 expression was measured by real-time PCR. Data are presented as mean±SEM. *: p<0.05. 3T3-L1 adipocytes treated with IH or control were stimulated with or without insulin 100 nM for 30 min and whole-cell lysates were blotted for the indicated antibodies (c). n=3, shown is a representative blot and densitometry analysis; mean±SEM. *: p<0.05. Adipose explants of obese mice treated with IH or control were stimulated with or without insulin (100 nM) for 15 min and lysates were blotted for P-Akt, total Akt and β-actin (d). n=4 per group, shown is a representative blot and densitometry analysis for P-Akt/total Akt; mean±SEM. *: p<0.05.

characteristic feature of obese, metabolically dysfunctional adipose tissue is the formation of CLS, which consist of macrophages surrounding necrotic adipocytes [13]. Visceral adipose tissue in lean animals treated with IH demonstrated an increased amount of CLS compared with controls. Furthermore, there was a trend towards increased CLS in weight-matched obese mice; however, this failed to reach statistical significance (figure 3d and e). In terms of understanding the impact of IH on the adipose inflammatory phenotype, we found that conditioned media from adipose tissue explants from obese mice treated with IH induced greater activation of NF-κB than explants from control mice (figure 3f), and there was also a trend towards greater NF-κB activation with IH in lean mice (p=0.097). To further understand whether macrophage polarisation is directly caused by IH, we treated THP1-derived macrophages with IH or control *in vitro*. The classical protocol for M1 polarisation involves macrophage incubation in the presence of IFN-γ or LPS and to measure the expression of several classical M1 characterising genes such as tumour necrosis factor-α, interleukin (IL)-8 or IL-6 [19, 20]. IH under basal conditions and in the presence of these stimuli increased mRNA expression of all three of these genes (figure 3g). These data support the findings obtained from mice studies, indicating that the adipose macrophage polarisation observed *in vivo* is directly caused by IH.

Thus, these *in vivo* and *in vitro* data demonstrate that IH induces a pro-inflammatory phenotype in adipose tissue that in obesity is known to correlate with metabolic dysfunction.

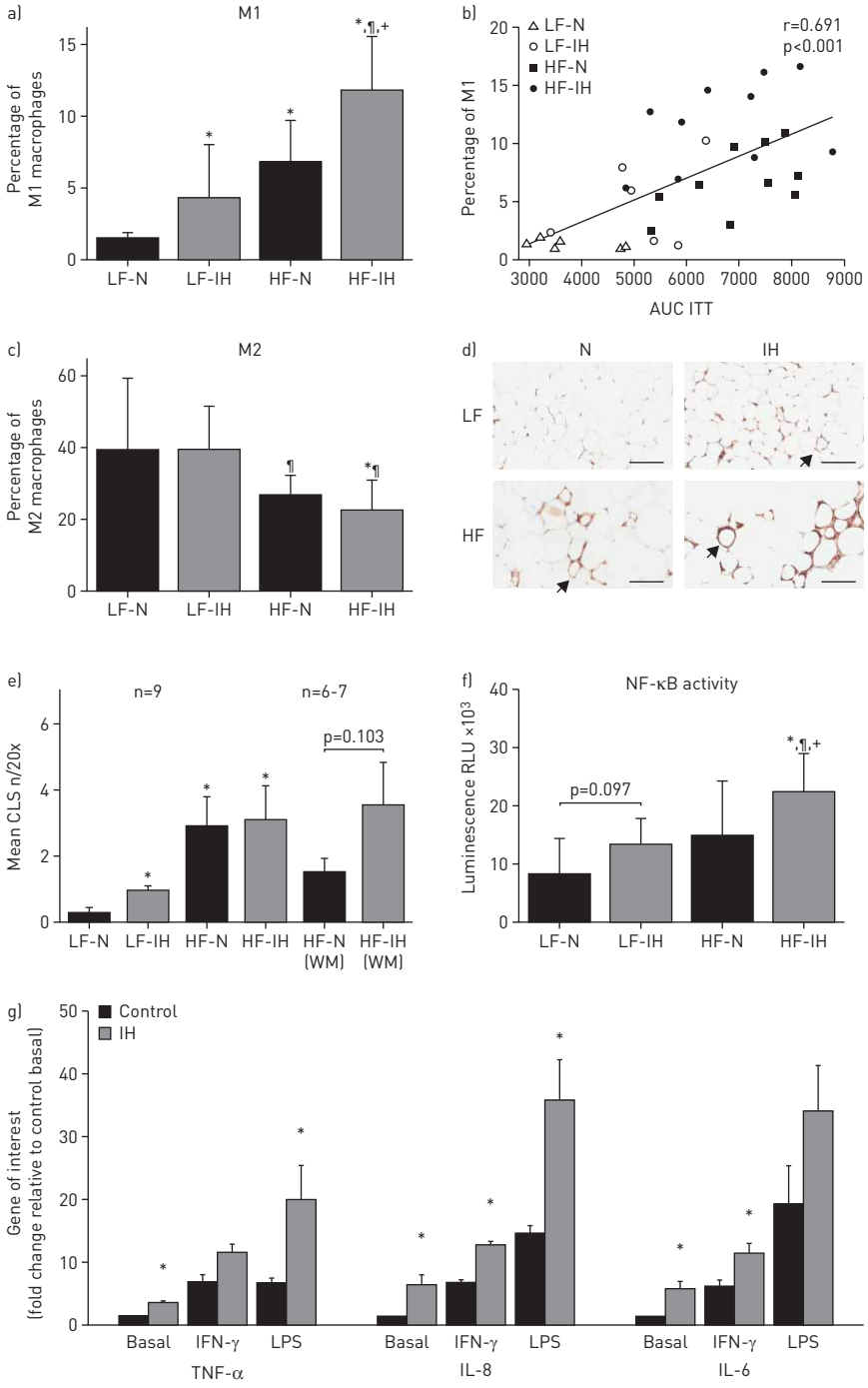

FIGURE 3 Intermittent hypoxia (IH) induces a pro-inflammatory phenotype in visceral epididymal adipose tissue (EAT) in lean and obese mice and polarises THP1-derived macrophages towards a M1 pro-inflammatory phenotype. Lean (LF) and diet-induced obese (HF) mice were treated with IH or control (N) for 6 weeks. Stromal vascular fraction of the EAT was obtained (LF, n=6; HF, n=10 per group) and recruitment of adipose tissue macrophages (ATM) were determined by flow cytometry. Cells double positive ($F4/80^+/CD11B^+$) were characterised as ATM. Of these, percentage of M1 macrophages ($F4/80^+/CD11B^+/CD11C^+/Cd206^{dim}$) was monitored (a) and correlated to the level of insulin resistance as determined by insulin tolerance test (ITT) (b). Percentage of M2 macrophages ($F4/80^+/CD11B^+/CD11C^-/Cd206^{bright}$) was also evaluated (c). Data are presented as mean±SD. *: p<0.05 *versus* LF-N; ¶: p<0.05 *versus* LF-IH; $^+$: p<0.05 *versus* HF-N. Furthermore, we investigated the presence of crown-like structures (CLS) by F4/80 immunohistochemistry (d) shown are representative images, arrows indicate CLS. Scale bars=100 µm. CLS density was determined by counting of CLS in 10 random high-power fields (20×) (e) and results are represented for un-matched and weight-matched animals (HF mice). Data are presented as mean±SEM. *: p<0.05 *versus* LF-N. Next, we investigated the pro-inflammatory signature of the adipose tissue. Adipose explants (50 mg) obtained following treatment with IH or control were cultured *ex vivo* for 24 h. Media was harvested and incubated with NIH-3T3-NF-κB luciferase cells for 16 h at 37°C before luminescence was measured (f) Data are presented as mean±SD. *: p<0.05 *versus* LF-N; ¶: p<0.05 *versus* LF-IH; $^+$: p<0.05 *versus* HF-N. LF, n=7; HF, n=10–12 per group. In order to test the direct effect of IH on macrophage polarisation, THP1-derived macrophages were treated with IH or control and for the last 24 h were incubated in RPMI medium (basal) or stimulated with interferon (IFN)-γ (20 ng·mL^{-1}) or lipopolysaccharide LPS (1 µg·mL^{-1}). mRNA was harvested and reverse transcribed before real-time PCR of M1-characteristic genes. Data are presented as mean±SEM. *p<0.05, IH *versus* control; n=3–6 (g). AUC: areas under the curve; TNF: tumour necrosis factor; IL: interleukin.

OSA is independently associated with IR

As a next step, we investigated the potential role of the findings obtained from the murine and *in vitro* models of IH for patients with OSA. Several studies have suggested an association of OSA and IR; however, uncertainty remains if this relationship persists in obese subjects. To gain further insight into this subject, we employed a cross-sectional cohort of carefully selected subjects with a specific focus on the interaction of OSA with obesity. A total of 186 male subjects without pre-existing cardiovascular and metabolic disorders were recruited from the Pulmonary Sleep Disorders Unit of St Vincent's University Hospital, Dublin, Ireland, (n=152) and from the Sleep Laboratory at the University of Grenoble, France (n=34). Subjects were classified into three different weight groups (group 1, lean/overweight (body mass index (BMI) <30 $kg \cdot m^{-2}$); group 2, obesity class 1 (BMI ⩾30 and <35); group 3, obesity class ⩾2 (BMI ⩾35)) and within these groups into subjects without (A) and with (B) OSA (table 2). BMI and the waist/hip ratio were similar in OSA and controls within all three weight categories, but HOMA-IR values were higher in OSA patients than controls, although in group 3 this difference failed to reach statistical significance (p=0.07) (figure 4). Pearson's correlation analysis showed that HOMA-IR correlated most strongly with BMI (r=0.539, p<0.001), oxygen desaturation index (ODI) (r=0.406, p<0.001) and apnoea/hypopnoea index (AHI) (r=0.405, p<0.001). Stepwise multiple linear regression analysis identified BMI (β=0.421, p<0.001) and the OSA severity markers AHI (β=0.228, p=0.004) and ODI (when this last value was entered instead of AHI, β=0.239, p=0.004) as independent predictors of HOMA-IR.

Thus, OSA contributes to IR in men without cardiovascular and metabolic comorbidities independently of the degree of obesity.

The circulating marker of macrophage activation and polarisation sCD163 correlates significantly and independently with OSA severity

As outlined above, we demonstrated that IH induces ATM polarisation towards an M1 phenotype in lean and obese mice and also in cultured THP-1-derived macrophages. To investigate the potential role of these findings for subjects with OSA, we next measured serum levels of CD163, an established marker of macrophage activation and M1 polarisation, in our patient cohort (n=149). We found a significant correlation between sCD163 and OSA severity (figure 5), and in linear regression, adjusted for anthropometric and demographic parameters, the AHI (or ODI when substituted for AHI) remained the only significant predictor of this response (β=0.369, p<0.001).

Thus, OSA severity correlates significantly with sCD163, suggesting M1 macrophage polarisation in OSA patients.

TABLE 2 Baseline characteristics of human population

	Group 1A	Group 1B	Group 2A	Group 2B	Group 3A	Group 3B
	BMI <30, control	BMI <30, OSA	BMI >30, <35, control	BMI >30, <35, OSA	BMI >35, control	BMI >35, OSA
Subjects n	35	42	23	34	9	43
Age years	44±10	45±9	40±7	43±8	38±8	43±9
BMI $kg \cdot m^{-2}$	**26.7±2.0**	**27.0±2.3**	**32.1±1.4***	**32.2±1.3***	**38.6±3.9*,¶**	**40.8±4.6*,¶**
WHR	**0.94±0.06**	**0.94±0.06**	**1.01±0.05***	**1.01±0.05***	**1.03±0.05***	**1.04±0.05*,¶**
Smoking						
Current	6 (18%)	5 (12%)	4 (17%)	5 (17%)	0 (0%)	6 (14%)
Ex-smoker	5 (15%)	18 (44%)	9 (39%)	10 (34%)	5 (56%)	12 (28%)
Pack-years	4±8	6±10	8±11	8±12	9±9	8±12
ESS	**8±6**	**10±6**	**10±6**	**12±5**	**9±7**	**12±5#**
AHI	**4.0±2.8**	**28.5±17.7+**	**4.0±2.8**	**37.7±21.9+**	**3.1±1.3**	**48.0±25.5+,§**
ODI	**2.3±2.1**	**22.3±14.5+**	**3.4±2.3**	**33.0±20.4+**	**2.8±1.1**	**44.9±26.1+,§**
Basal S_{aO_2}	95±1	94±4	94±2	94±1+	94±2	93±2
Min S_{aO_2}	**90±3**	**83±6+**	**88±2**	**79±8+**	**88±4**	**75±11+,§**
TST <90%	**0±1**	**5±10**	**0±1**	**8±15**	**1±2**	**21±23##**
Fasting glucose $mmol \cdot L^{-1}$	5.0±0.4	5.0±0.5	5.2±0.7	5.8±2.1*	5.3±0.7	5.5±0.9
Fasting insulin $mU \cdot L^{-1}$	**6.8±4.3**	**10.2±9.2+**	**13.1±4.9#**	**17.3±11.7***	**20.2±8.4*,f**	**24.4±11.8*,¶**
Total cholesterol $mmol \cdot L^{-1}$	**4.1±1.6**	**3.5±1.7**	**4.9±0.6§**	**4.9±0.8§**	**5.3±1.0§**	**4.8±0.8§**
HDL-cholesterol $mmol \cdot L^{-1}$	**1.24±0.31**	**1.32±0.36**	**1.03±0.18§**	**1.09±0.27§**	**1.11±0.13**	**1.02±0.27***
LDL-cholesterol $mmol \cdot L^{-1}$	**2.44±1.37**	**1.73±1.51**	**3.12±0.58§**	**3.03±0.71§**	**3.41±0.91§**	**2.82±0.79§**
Triglyceride $mmol \cdot L^{-1}$	1.63±1.82	1.30±0.64	1.67±0.74	1.79±1.02	1.67±0.45	1.95±1.33

Data are presented as mean±SD, unless otherwise stated. Bold represents significantly different parameters. BMI: body mass index; WHR: waist/hip ratio; ESS: Epworth Sleepiness Scale; AHI: apnoea/hypopnoea index; ODI: oxygen desaturation index; S_{aO_2}: mean nocturnal oxygen saturation; TST <90%: per cent of total sleep time with oxygen saturation <90%; HDL: high-density lipoprotein; LDL: low-density lipoprotein. *: p<0.05 *versus* group 1A+B; ¶: p<0.05 *versus* group 2A+B; #: p<0.05 *versus* group 1A; +: p<0.05 *versus* control; §: p<0.05 *versus* group 1B; f: p<0.05 *versus* group 2A; ##: p<0.05 *versus* all other groups.

Discussion

In this report we provide evidence from cell culture, murine and human studies that IH in OSA contributes independently to the development of IR. We also demonstrate for the first time that IH induces obesity-like morphological pro-inflammatory changes in adipose tissue, which correlate with IR in lean and obese mice and may contribute to the pathogenesis of IR in patients with OSA.

The results of our study are in keeping with previous reports [4–6, 8, 21] supporting an independent association of OSA with IR. These findings are strengthened by the exclusion of subjects with significant confounding comorbidities, and the recruitment of participants across the spectrum of weight categories. We believe that the lack of statistical significance in HOMA-IR between OSA and controls in group 3 is due to the low number of controls, subjects which are especially difficult to recruit; overall, our data indicate that OSA impacts on IR independently of the degree of obesity.

The pivotal role of IH in the underlying pathogenesis is supported by the mouse experiments demonstrating diminished insulin sensitivity with IH. Previous studies have mainly been performed in lean mice [17, 22–25]. Drager *et al.* [23] also reported impaired insulin sensitivity in diet-induced obese mice using the HOMA-IR index as a surrogate marker that remained unaffected by IH in our experiments. This parameter reflects the balance between hepatic glucose output and insulin secretion, which is maintained by a feedback loop between the liver and β-cells, unlike the ITT, which also assesses the peripheral insulin sensitivity of the target tissues, *i.e.* adipose tissue and skeletal muscle [26]. In rodents, the HOMA-IR index is less sensitive to changes in insulin sensitivity [27] and whereas Drager *et al.* [23] measured fasting glucose and insulin directly after cessation of IH, we performed these measurements after overnight cessation of the stimulus, which may explain the discrepancy between the two studies.

Although the detailed pathophysiological sequences underlying IH-mediated metabolic dysfunction still need to be defined, our study provides novel insight into the mechanisms by which IH contributes to IR. We reported previously that IH induces morphological and inflammatory remodelling of visceral adipose tissue in lean mice [17] and a profound pro-inflammatory response in cultured adipocytes [16], and we demonstrate here that these events lead to IR associated with downregulation of the insulin signalling pathway. In obesity, changes in the cellular composition of the stromal–vascular fraction towards a pro-inflammatory phenotype are a key component of metabolically dysfunctional adipose tissue. The polarisation of macrophages towards an M1, pro-inflammatory subtype leading to the generation of multiple pro-inflammatory factors plays a pivotal role in this setting [13]. We demonstrate that even in lean mice, IH induces typical obesity-like morphological changes of the adipose tissue, with significant increases in M1 macrophages, confirming data by Carreras *et al.* [22] using a similar protocol. In obese mice, IH potentiates these pro-inflammatory changes, despite IH leading to significant weight loss in these

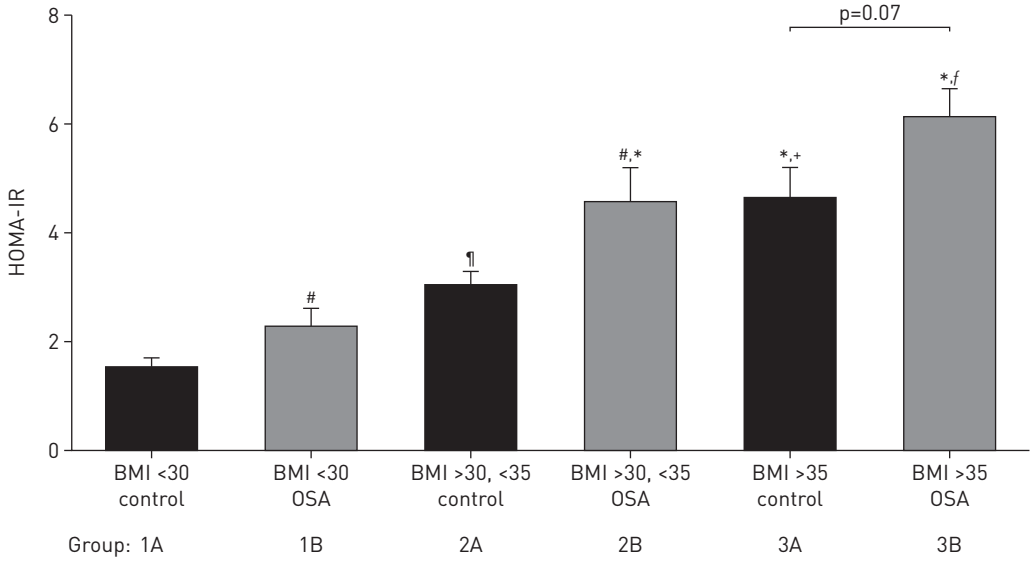

FIGURE 4 Obstructive sleep apnoea (OSA) is independently associated with insulin resistance (IR). HOMA-IR index in subjects of three different weight categories without (groups 1A, 2A and 3A) and with OSA (groups 1B, 2B and 3B) free of any cardiovascular or metabolic comorbidities were calculated. Data are presented as mean±SEM. #: p<0.05 *versus* control; ¶: p<0.05 *versus* group 1A; *: p<0.05 *versus* group 1A+B; +: p<0.05 *versus* group 2A; *f*: p<0.05 *versus* group 2A+B. BMI: body mass index.

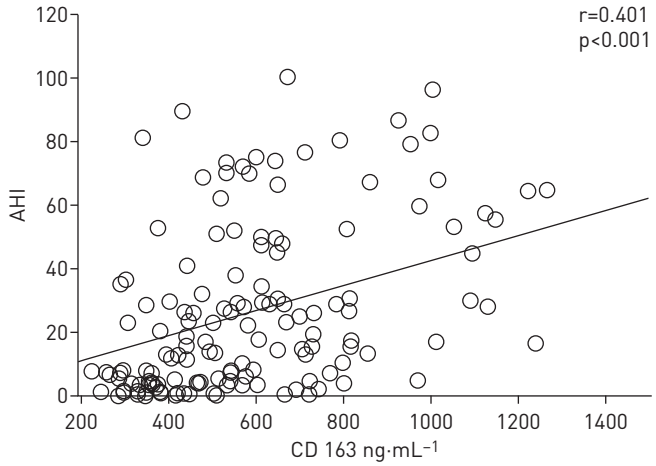

FIGURE 5 Obstructive sleep apnoea (OSA) severity as determined by the apnoea/hypopnoea index (AHI) correlates significantly and independently with serum levels of sCD163. To determine the potential role of adipose tissue macrophages polarisation towards an M1 pro-inflammatory phenotype in patients with OSA, we measured circulating serum levels of CD163, an established marker of macrophage activation and M1 polarisation, in OSA patients and controls *via* ELISA (n=149). Correlation of sCD163 with OSA severity as determined by apnoea/hypopnoea index (AHI) is demonstrated.

animals. Differences in insulin sensitivity only became significant after adjustment for IH-related weight loss, perhaps reflecting the effect of obesity on IR in other target organs, such as skeletal muscle. Weight loss in response to IH is a well-described confounding finding [23, 28] and is due to a combination of decreased food intake and altered energy expenditure. Pair-feeding would only partly resolve this issue and, hence, provides limited benefit. Supporting the conclusion that the adipose tissue changes were due to the direct effects of IH treatment are the changes seen in lean mice, where no difference in body and adipose tissue weight was observed between mice exposed to IH and controls, and from the cell culture studies demonstrating M1 macrophage polarisations of THP1 cells in response to IH.

As a novel finding of our study, we established a significant correlation of OSA severity with sCD163 as an emerging marker of M1 macrophage polarisation in humans. Although a definitive direct connection between the increased sCD163 levels observed in OSA patients and the adipose tissue as a source cannot be drawn at this stage, the results from the animal model nonetheless suggest that this may be the case. In support of this hypothesis, a recent study demonstrated a significant correlation of sCD163 with CD163 expression in adipose tissue [29]. CD163 is expressed on M2 macrophages but to become soluble requires cleavage by ADAM-17, which is dependent on M1 macrophages [30]. Hence, sCD163 has increasingly been linked to adipose tissue inflammation in insulin resistance and T2D, and is an emerging pro-inflammatory biomarker of various cardiovascular diseases [31–34]. This is the first study investigating sCD163 in OSA and strongly supports evidence of macrophage polarisation in this condition. Its detailed role in OSA and the link directly to metabolic and cardiovascular disease processes will, however, require further targeted evaluation including large prospective studies.

Our study has significant strengths including the comprehensive translational nature of the study, which includes a carefully selected patient cohort, an animal model that includes the evaluation of lean and obese mice, and a state-of-the art *in vitro* model of IH. Previous cell culture models of IH have been limited by requiring prolonged soak times, reduced cycle numbers and inadequate control treatment. Here, the oxygen desaturation patterns closely resemble those observed in OSA and, thus, this model is far superior to previous reported models. Campillo *et al.* [35] have recently described a similar model . However, we acknowledge that the IH pattern may differ substantially in various tissues. One study using a murine model suggested that the oxygen fluctuations of IH are attenuated in adipose tissue [36]. However, how this relates to human adipose tissue is unknown and it is likely that there will be significant local differences within the tissue depending on the relative distance to the circulatory system. Notably, our findings obtained *in vitro* closely resembled the animal data supporting the suitability of this model for adipocytes; however, further targeted studies are required.

One potential limitation of our study is the sole focus on the adipose tissue, but we acknowledge that other organs are likely to be involved in the pathogenesis of IR. IH also contributes to steatohepatitis [37, 38] and may also have a detrimental effect on β-cell function [25]. Further studies will need to define the detailed contribution of these adverse actions in glucose metabolic dysfunction. Moreover, we did not investigate the potential contribution of other WAT compartments in mice other than EAT, such as the subcutaneous and

mesenteric fraction. In cell culture, human primary subcutaneous and visceral adipocytes have similar pro-inflammatory potential in response to IH [16], but it remains unknown if other parts of WAT behave similarly to EAT *in vivo*. A further potential limitation is the exclusion of female OSA patients. We designed the study specifically in this way to avoid gender differences that could influence the analysis. However, as a consequence, our data cannot be extrapolated to women.

In conclusion, this study provides evidence of pro-inflammatory changes of the adipose tissue in response to IH that may be a crucial link between OSA and the development of IR.

References

1 Ryan S, Crinion SJ, McNicholas WT. Obesity and sleep-disordered breathing when two 'bad guys' meet. *QJM* 2014; 107: 949–954.
2 McNicholas WT, Bonsignore MR. Sleep apnoea as an independent risk factor for cardiovascular disease: current evidence, basic mechanisms and research priorities. *Eur Respir J* 2007; 29: 156–178.
3 Lévy P, Kohler M, McNicholas WT, *et al.* Obstructive sleep apnoea syndrome. *Nat Rev Dis Primers* 2015; 1: 15015.
4 Ip MS, Lam B, Ng MM, *et al.* Obstructive sleep apnea is independently associated with insulin resistance. *Am J Respir Crit Care Med* 2002; 165: 670–676.
5 Kent BD, Grote L, Ryan S, *et al.* Diabetes mellitus prevalence and control in sleep-disordered breathing: the European Sleep Apnea Cohort (ESADA) study. *Chest* 2014; 146: 982–990.
6 Punjabi NM, Sorkin JD, Katzel LI, *et al.* Sleep-disordered breathing and insulin resistance in middle-aged and overweight men. *Am J Respir Crit Care Med* 2002; 165: 677–682.
7 Kent BD, McNicholas WT, Ryan S. Insulin resistance, glucose intolerance and diabetes mellitus in obstructive sleep apnoea. *J Thorac Dis* 2015; 7: 1343–1357.
8 Pamidi S, Wroblewski K, Stepien M, *et al.* Eight hours of nightly continuous positive airway pressure treatment of obstructive sleep apnea improves glucose metabolism in patients with prediabetes. A randomized controlled trial. *Am J Respir Crit Care Med* 2015; 192: 96–105.
9 Ryan S, McNicholas WT. Intermittent hypoxia and activation of inflammatory molecular pathways in OSAS. *Arch Physiol Biochem* 2008; 114: 261–266.
10 Ryan S, Taylor CT, McNicholas WT. Selective activation of inflammatory pathways by intermittent hypoxia in obstructive sleep apnea syndrome. *Circulation* 2005; 112: 2660–2667.
11 Ryan S, Taylor CT, McNicholas WT. Predictors of elevated nuclear factor-κB-dependent genes in obstructive sleep apnea syndrome. *Am J Respir Crit Care Med* 2006; 174: 824–830.
12 Arnaud C, Beguin PC, Lantuejoul S, *et al.* The inflammatory preatherosclerotic remodeling induced by intermittent hypoxia is attenuated by RANTES/CCL5 inhibition. *Am J Respir Crit Care Med* 2011; 184: 724–731.
13 Ouchi N, Parker JL, Lugus JJ, *et al.* Adipokines in inflammation and metabolic disease. *Nat Rev Immunol* 2011; 11: 85–97.
14 Trayhurn P, Wang B, Wood IS. Hypoxia and the endocrine and signalling role of white adipose tissue. *Arch Physiol Biochem* 2008; 114: 267–276.
15 Pasarica M, Sereda OR, Redman LM, *et al.* Reduced adipose tissue oxygenation in human obesity: evidence for rarefaction, macrophage chemotaxis, and inflammation without an angiogenic response. *Diabetes* 2009; 58: 718–725.
16 Taylor CT, Kent BD, Crinion SJ, *et al.* Human adipocytes are highly sensitive to intermittent hypoxia induced NF-κB activity and subsequent inflammatory gene expression. *Biochem Biophys Res Commun* 2014; 447: 660–665.
17 Poulain L, Thomas A, Rieusset J, *et al.* Visceral white fat remodelling contributes to intermittent hypoxia-induced atherogenesis. *Eur Respir J* 2014; 43: 513–522.
18 Guo S. Insulin signaling, resistance, and the metabolic syndrome: insights from mouse models into disease mechanisms. *J Endocrinol* 2014; 220: T1–T23.
19 Daigneault M, Preston JA, Marriott HM, *et al.* The identification of markers of macrophage differentiation in PMA-stimulated THP-1 cells and monocyte-derived macrophages. *PLoS One* 2010; 5: e8668.
20 Italiani P, Boraschi D. From monocytes to M1/M2 macrophages: phenotypical vs. functional differentiation. *Front Immunol* 2014; 5: 514.
21 Iftikhar IH, Hoyos CM, Phillips CL, *et al.* Meta-analyses of the Association of Sleep Apnea with insulin resistance, and the effects of CPAP on HOMA-IR, adiponectin, and visceral adipose fat. *J Clin Sleep Med* 2015; 11: 475–485.
22 Carreras A, Zhang SX, Almendros I, *et al.* Resveratrol attenuates intermittent hypoxia-induced macrophage migration to visceral white adipose tissue and insulin resistance in male mice. *Endocrinology* 2015; 156: 437–443.
23 Drager LF, Li J, Reinke C, *et al.* Intermittent hypoxia exacerbates metabolic effects of diet-induced obesity. *Obesity* 2011; 19: 2167–2174.
24 Iiyori N, Alonso LC, Li J, *et al.* Intermittent hypoxia causes insulin resistance in lean mice independent of autonomic activity. *Am J Respir Crit Care Med* 2007; 175: 851–857.
25 Polak J, Shimoda LA, Drager LF, *et al.* Intermittent hypoxia impairs glucose homeostasis in C57BL6/J mice: partial improvement with cessation of the exposure. *Sleep* 2013; 36: 1483–1490.
26 Wallace TM, Levy JC, Matthews DR. Use and abuse of HOMA modeling. *Diabetes Care* 2004; 27: 1487–1495.
27 Lee S, Muniyappa R, Yan X, *et al.* Comparison between surrogate indexes of insulin sensitivity and resistance and hyperinsulinemic euglycemic clamp estimates in mice. *Am J Physiol Endocrinol Metab* 2008; 294: E261–E270.
28 Poulain L, Richard V, Lévy P, *et al.* Toll-like receptor-4 mediated inflammation is involved in the cardiometabolic alterations induced by intermittent hypoxia. *Mediators Inflamm* 2015; 2015: 620258.
29 Kračmerová J, Rossmeislová L, Kováčová Z, *et al.* Soluble CD163 is associated with CD163 mRNA expression in adipose tissue and with insulin sensitivity in steady-state condition but not in response to calorie restriction. *J Clin Endocrinol Metab* 2014; 99: E528–E535.
30 Etzerodt A, Maniecki MB, Møller K, *et al.* Tumor necrosis factor alpha-converting enzyme (TACE/ADAM17) mediates ectodomain shedding of the scavenger receptor CD163. *J Leukoc Biol* 2010; 88: 1201–1205.
31 Moreno JA, Dejouvencel T, Labreuche J, *et al.* Peripheral artery disease is associated with a high CD163/TWEAK plasma ratio. *Arterioscler Thromb Vasc Biol* 2010; 30: 1253–1262.

32 Sørensen LP, Parkner T, Søndergaard E, *et al.* Visceral obesity is associated with increased soluble CD163 concentration in men with type 2 diabetes mellitus. *Endocr Connect* 2015; 4: 27–36.
33 Subramanian S, Tawakol A, Burdo TH, *et al.* Arterial inflammation in patients with HIV. *JAMA* 2012; 308: 379–386.
34 Urbonaviciene G, Martin-Ventura JL, Lindholt JS, *et al.* Impact of soluble TWEAK and CD163/TWEAK ratio on long-term cardiovascular mortality in patients with peripheral arterial disease. *Atherosclerosis* 2011; 219: 892–899.
35 Campillo N, Jorba I, Schaedel L, *et al.* A novel chip for cyclic stretch and intermittent hypoxia cell exposures mimicking obstructive sleep apnea. *Front Physiol* 2016; 7: 319.
36 Reinke C, Bevans-Fonti S, Drager LF, *et al.* Effects of different acute hypoxic regimens on tissue oxygen profiles and metabolic outcomes. *J Appl Physiol* 2011; 111: 881–890.
37 Aron-Wisnewsky J, Minville C, Tordjman J, *et al.* Chronic intermittent hypoxia is a major trigger for non-alcoholic fatty liver disease in morbid obese. *J Hepatol* 2012; 56: 225–233.
38 Savransky V, Bevans S, Nanayakkara A, *et al.* Chronic intermittent hypoxia causes hepatitis in a mouse model of diet-induced fatty liver. *Am J Physiol Gastrointest Liver Physiol* 2007; 293: G871–G877.